Available online at www.sciencedirect.com
SCIENCE DIRECT®
Thin Solid Films 436 (2003) 273–276
thin solid films
www.elsevier.com/locate/tsf

# Correlation of Raman and X-ray diffraction measurements of annealed pulsed laser deposited ZnO thin films

C. Roy[a], S. Byrne[a], E. McGlynn[a,*], J.-P. Mosnier[a], E. de Posada[b], D. O'Mahony[b], J.G. Lunney[b], M.O. Henry[a], B. Ryan[a], A.A. Cafolla[c]

[a]*School of Physical Sciences/National Centre for Plasma Science and Technology, Dublin City University, Glasnevin, Dublin 9, Ireland*
[b]*Physics Department, Trinity College Dublin, Dublin 2, Ireland*
[c]*School of Physical Sciences/National Centre for Sensor Research, Dublin City University, Glasnevin, Dublin 9, Ireland*

Received 5 November 2002; received in revised form 12 March 2003; accepted 13 April 2003

**Abstract**

Raman spectroscopy, X-ray diffractometry and atomic force microscopy have been used to characterise ZnO thin films grown by pulsed laser deposition as a function of the post-growth annealing temperature. The results show substantial enhancement and broadening of certain Raman features which correlate excellently with the change in width of the X-ray diffraction peaks. The 570 $cm^{-1}$ Raman feature showed pronounced asymmetry and enhanced intensity in the unannealed sample. An increase in grain size observed after subsequent annealing produced a substantial reduction in both the asymmetry and intensity of this peak. Our experimental data suggest that electric fields, due to charge trapping at grain boundaries, in conjunction with localised and surface phonon modes are the cause of the intensity enhancement and asymmetry of this feature.


*PACS:* 81.15.Fg; 78.66.Hf; 68.55.Jk; 68.60.Dv

*Keywords:* Laser deposition; II–VI semiconductors; Structure and morphology; Thermal effects

## 1. Introduction

Recent years have seen a renewed interest in the II–VI semiconductor ZnO (direct bandgap approx. 3.3 eV). ZnO crystallises in the wurzite lattice, is optically transparent with a large exciton binding energy of 60 meV, and is capable of UV emission and lasing. ZnO is normally n-type, but p-type ZnO has been grown which has contributed significantly to the fabrication of UV/blue LEDs and laser diodes. Recently, ZnO nanowires have shown UV lasing under optical pumping, and fabrication of a homostructural ZnO p–n junction has been reported (see, e.g. Refs. [1–3]).

In this study, Raman Spectroscopy and X-ray diffraction (XRD) were employed to characterise thin films grown using pulsed laser deposition (PLD) and annealed in situ at various temperatures. Our data allow us to firmly identify the mechanism responsible for enhancement of the 570 $cm^{-1}$ Raman feature observed in polycrystalline samples.

## 2. Experimental details

ZnO films were grown on (0001) sapphire substrates by PLD using a 10 Hz pulsed KrF excimer laser ($\lambda =$ 248 nm). The fluence on target was set at 1.7 $J/cm^2$ for all samples. A ZnO ceramic target (99.99%) was used throughout. The target to substrate distance was ~4 cm. The thin films were grown in an $O_2$ (purity 99.99%) pressure of 0.3 mbar and the substrate temperature was maintained at 400 °C during growth. Typically the films were 150–200 nm, giving a deposition rate of 0.025 nm/pulse. The films were subsequently annealed in $O_2$ (0.3 mbar) between 400 and 600 °C (see Table 1) in the growth chamber immediately after deposition. SEM data show that the films are continuous and show

*Corresponding author. Tel.: +353-17005387; fax: +353-17005384.
*E-mail address:* enda.mcglynn@dcu.ie (E. McGlynn).

0040-6090/03/$ - see front matter © 2003 Elsevier Science B.V. All rights reserved.
doi:10.1016/S0040-6090(03)00617-5

Table 1
Growth conditions and results of X-ray analysis for our PLD-grown ZnO thin films

| Sample | Annealing temp. (°C) | Annealing time (min) | FWHM of (0002) peak (°) | Average grain size (nm) |
|---|---|---|---|---|
| a | No anneal | – | 0.34 | 32 |
| b | 400 | 10 | 0.22 | 67 |
| c | 500 | 15 | 0.21 | 79 |
| d | 600 | 10 | 0.20 | 81 |

no evidence of porosity. The crystal structure and quality of the samples were investigated by XRD in the θ–2θ mode (Siemens D500 using Cu $K_\alpha$ radiation). Raman scattering measurements were performed using a micro-Raman spectrometer equipped with a CCD detector. Raman spectra were excited with 1.96 eV photons from a He–Ne laser ($\lambda \sim 633$ nm) or, for the resonance excitation measurements, with 3.82 eV photons from an UV laser ($\lambda = 325$ nm), in both cases using back scattering geometry. The He–Ne laser beam of 5–6 mW was focussed on the sample surface to a spot of diameter ~10 μm. Atomic force microscopy (AFM) measurements were made using a commercial AFM in contact mode operation.

## 3. Results

X-ray diffraction measurements as a function of annealing temperature are presented in Fig. 1. They are dominated by the (0002) and (0004) ZnO peaks along with the prominent (0006) sapphire peak. The dominance of the (0002) and (0004) peaks indicate that ZnO thin films highly textured along the (0001) direction have been grown [4]. The lattice parameters of the ZnO thin films perpendicular to the substrate can be calculated from the diffraction angles corresponding to the $(10\bar{1}0)$ and (0002) planes. The intensity of the $10\bar{1}0$ peak is small compared to the (0002) peak intensity due to the high degree of *c*-axis orientation. The average values of *c*- and *a*-axis lattice constants of our PLD samples are 0.518 nm and 0.330 nm, respectively, and the values for all samples were identical within the limits of our experimental accuracy (±0.001 nm). The average grain size (parallel to the (0002) direction) of the ZnO films can be estimated from the full width at half maximum (FWHM) of the (0002) peak using Scherrer's relation [5] (see Table 1). The range of annealing temperatures used in our work coincides with those known to lead to major grain growth [6,7]. The annealed samples show a decrease of (0002) peak FWHM and consequent increase in grain size with increasing annealing temperature. These results are supported by AFM imaging of the samples (Fig. 2), where measurements of the lateral grain sizes are 135±40 nm

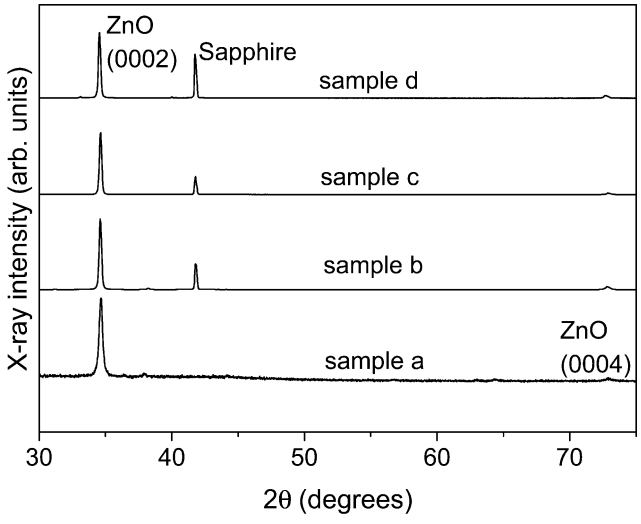


Fig. 1. θ–2θ XRD scans showing the (0002) and (0004) Bragg peaks obtained with the PLD-grown ZnO films: (a) unannealed; (b), (c) and (d) annealed at 400 °C, 500 °C and 600 °C, respectively.

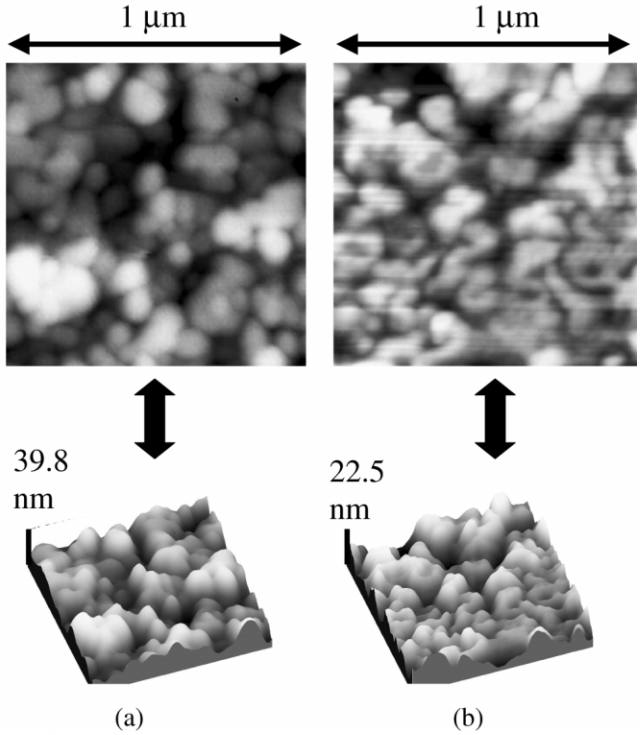


Fig. 2. AFM images of PLD-grown ZnO thin films: (a) annealed at 400 °C; (b) annealed at 500 °C. The average grain sizes estimated from these images are 135±40 nm for the sample annealed at 400 °C and 180±50 nm for the sample annealed at 500 °C.

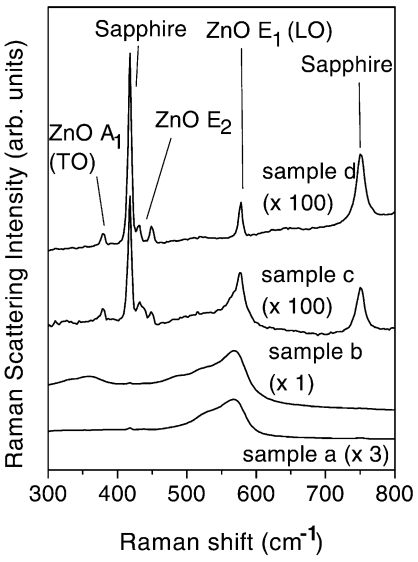


Fig. 3. Non-resonant ($\lambda_{exc}=632$ nm) Raman spectra of PLD grown ZnO thin films: (a) not annealed; (b), (c) and (d) annealed at 400 °C, 500 °C and 600 °C, respectively.

for the sample annealed at 400 °C and $180\pm50$ nm for the sample annealed at 500 °C. The annealing process clearly produces a recovery of the crystal structure and increase of the grain size. We note that in our experimental conditions, the increase in grain size is achieved after annealing for relatively short times. Such an effect was also observed in the case of magnetron sputtered ZnO [8].

The unpolarised Raman spectra (with He–Ne excitation) of the ZnO thin films are shown in Fig. 3 as a function of annealing temperature. The peaks at 418 and 751 $cm^{-1}$ are due to scattering from the sapphire substrate. The $E_2$ 437 $cm^{-1}$ peak, characteristic of the wurtzite lattice, can be seen in all samples. The $A_1$ (TO) mode at 379 $cm^{-1}$ is apparent in samples c and d. However, the Raman spectra are dominated by the longitudinal optical vibration at $\sim$570 $cm^{-1}$. This band is attributed to the $E_1$ (LO) mode [9]. The intensity and FWHM of the 570 $cm^{-1}$ peak appears anomalously high for the unannealed sample and the sample (b) which was annealed at 400 °C, but it is reduced dramatically (by a factor of 100 relative to the sapphire features) with increasing annealing temperature. In addition, this feature shows a marked asymmetry, which also decreases with increasing annealing temperature. Raman spectra were also measured with UV excitation $\lambda=325$ nm (or 3.82 eV) and are shown in Fig. 4. The spectra from all the samples are similar, that is the strong band at 570 $cm^{-1}$ was observed below the 800 $cm^{-1}$ spectral region whereas a 2LO vibrational mode at $\sim$1150 $cm^{-1}$ was recorded in the higher spectral range as reported by several authors [10,11]. The Raman peak at 570 $cm^{-1}$ is symmetric for all the PLD-grown ZnO samples when the excitation is at or above resonance.

## 4. Discussion

We observe a clear correlation between the XRD data and the corresponding non-resonant Raman spectra as a function of annealing temperature. As the average grain size increases, we observe a reduction in the relative intensity and asymmetry of the 570 $cm^{-1}$ band in the Raman spectra. The intensity and asymmetry of the LO mode at 570 $cm^{-1}$ has been widely discussed in the literature. Explanations for this structure include resonance enhancement due to impurity levels in the band gap [12], contributions from both the $A_1$ (LO) and $E_1$ (LO) modes due to random crystallite orientation [12] or a combination of electric field induced (EFI) Raman enhancement and one of the following mechanisms (i) coupled phonon-plasmon scattering or (ii) localised interface and/or surface phonon modes [13].

The absence of the characteristic second and higher order scattering in our spectra rules out the resonant enhancement by levels in the gap. These are observed in the spectra of the samples under UV excitation as expected. Contributions from both the $A_1$ (LO) and $E_1$ (LO) modes due to random crystallite orientation can also be ruled out for the reasons given by Exarhos and Sharma [12], namely that, after annealing the XRD

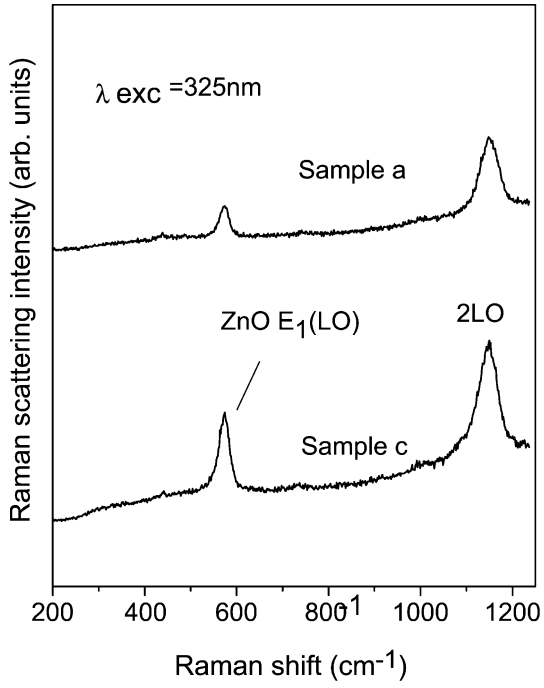


Fig. 4. Resonant ($\lambda_{exc}=325$ nm) Raman spectra of PLD grown ZnO thin films: (a) not annealed and (c) annealed at 500 °C. Similar spectra were obtained for the other samples. The 2LO feature characteristic of resonant Raman spectra is clearly seen at $\sim$1150 $cm^{-1}$.

results remain essentially the same, except for a reduction in the FWHM of the peaks, with no evidence for substantial crystallite reorientation. In addition, this cannot explain the abnormally high intensity of the 570 $cm^{-1}$ band in samples (a) and (b) in particular. Phonon–plasmon coupling is known to produce significant line shifts and broadening in Raman spectra. However, for highly polycrystalline material, the contribution of the lower frequency $L^-$ mode is generally absent, and a shift and broadening to higher energy of the $L^+$ mode is observed. This behaviour is not seen in our samples, hence we believe that the line broadening we observe is unlikely to be due to phonon–plasmon coupling.

The most consistent explanation of the behaviour of our Raman data is in terms of EFI enhancement (via charge trapping at grain boundaries) of the 570 $cm^{-1}$ feature [13]. This enhancement effect in conjunction with the presence of localised/surface phonon modes, which arise due to the small grain size, accounts for both the intensity and asymmetry of the peak in the unannealed sample [13]. Surface phonon modes have been reported at $\sim$550 $cm^{-1}$ in ZnO [14], which is close to the low energy side of the broad LO mode. In the annealed samples, the increase in the grain size reduces the grain boundary density and hence the effects of charge trapping at grain boundaries. Consequently the EFI enhancement is substantially reduced, in addition to elimination of the surface/interface modes. The importance of band bending at grain boundaries in polycrystalline samples and the presence of strong electric fields has also been found in studies of varistor action in ZnO [15] and of the green luminescence mechanism [16]. Similar enhancement and asymmetry effects have also been observed in the Raman scattering of ZnO containing gold colloids [17]. These were attributed to a surface enhancement effect caused by anomalously large electric fields due to the colloid plasmon resonance. Thus, our data appear to support the model proposed in Ref. [13]. This suggests that the enhancement and asymmetry of the 570 $cm^{-1}$ Raman feature of polycrystalline ZnO constitute a good indicator of the grain size of the material.

## 5. Conclusion

Pulsed laser deposited ZnO thin films have been characterised using X-ray diffractometry and Raman spectroscopy. All films show dominant *c*-axis orientation. The evolution of the FWHM of the XRD (0002) peaks with annealing temperature indicates an increase in the polycrystalline grain size which is confirmed by AFM measurements. A strong correlation between the enhancement and asymmetry of the 570 $cm^{-1}$ Raman mode and the FWHM of the XRD data has been observed. The presence of electric fields, due to charge trapping at grain boundaries, in addition to localised and surface phonon modes explains the intensity enhancement and asymmetry of the LO mode in the unannealed sample. An increase in the grain size and reduction in the electric field intensity due to annealing lead to a decrease in the intensity and asymmetry of the LO mode.

## Acknowledgments

The authors wish to acknowledge financial support provided by the Enterprise Ireland Basic Research Grants programme, and the financial support of the Higher Education Authority through the PRTLI programme.

## References

[1] Y.R. Ryu, S. Zhu, D.C. Look, J.M. Wrobel, H.M. Jeong, H.W. White, J. Cryst. Growth 216 (2000) 330.
[2] M.H. Huang, S. Mao, H. Feick, H. Yan, Y. Wu, H. Kind, E. Weber, R. Russo, P. Yang, Science 292 (2001) 1897.
[3] X. Guo, J. Choi, H. Tabata, T. Kawai, Jpn. J. Appl. Phys. 40 (2001) L177.
[4] T. Oshima, R.K. Thareja, Y. Yamagata, T. Ikegami, K. Ebihara, J. Narayan, Sci. Tech. Adv. Mater. 2 (2001) 517.
[5] B.D. Cullity, Elements of X-ray Diffraction, 2nd, Addison-Wesley, 1978.
[6] S.H. Bae, S.Y. Lee, H.Y. Kim, S. Im, Opt. Mater. 17 (2001) 327.
[7] V. Gupta, A. Mansingh, J. Appl. Phys. 80 (1996) 1063.
[8] M.K. Puchert, P.Y. Timbrell, R.N. Lamb, J. Vac. Sci. Technol. A 14 (1996) 2220.
[9] C.A. Arguello, D.L. Rousseau, S.P.S. Porto, Phys. Rev. 181 (1969) 1351.
[10] X.T. Zhang, Y.C. Liu, Z.Z. Zhi, J.Y. Zhang, Y.M. Lu, D.Z. Shen, W. Xu, G.Z. Zhong, X.W. Fan, X.G. Kong, J. Phys. D: Appl. Phys. 34 (2001) 3430.
[11] J.F. Scott, Phys. Rev. B 2 (1970) 1209.
[12] G.J. Exarhos, S.K. Sharma, Thin Solid Films 270 (1995) 27.
[13] M. Tzolov, N. Tzenov, D. Dimova-Malinovska, M. Kalitzova, C. Pizzuto, G. Vitali, G. Zollo, I. Ivanov, Thin Solid Films 379 (2000) 28.
[14] H. Ibach, Phys. Rev. Lett. 24 (1970) 1416.
[15] G.D. Mahan, J. Appl. Phys. 54 (1983) 3825.
[16] K. Vanheusden, W.L. Warren, C.H. Seager, D.R. Tallant, J.A. Voight, B.E. Gnade, J. Appl. Phys. 79 (1996) 7983.
[17] B.J. Bozlee, G.J. Exarhos, Thin Solid Films 377–378 (2000) 1.